




Concentric Circles and Spiral Configurations for Large Correlator Arrays in Radio Astronomy

Shahideh Kiehadrouinezhad¹ , Michael Cada^{1,2}, Zhizhang (David) Chen¹, Adib Shahabi¹, C. Ian Short³,
Zamri Zainal Abidin⁴, and Samiramis Kiehadrouinezhad^{5,6}

¹ Department of Electrical and Computer Engineering, Faculty of Engineering Dalhousie University, 5248 Morris Street, Halifax Canada; adib.shahabi@dal.ca

² The Nanotechnology Centre and IT4I, VSB—Technical University of Ostrava, 708 33 Ostrava-Poruba, Czech Republic

³ Department of Astronomy and Physics Saint Mary's University, Halifax Canada

⁴ Department of Physics, Science Faculty, University of Malaya, 50603 Kuala Lumpur, Malaysia

⁵ Department of Physics, Eberhad-Karls-Universität Tübingen Auf der Morgenstelle 14, D-72076 Tübingen, Germany

⁶ Institut of Astronomy and Astrophysics Department of Astronomy Sand 1, D-72076 Tübingen, Germany

Received 2018 July 3; revised 2018 August 22; accepted 2018 August 30; published 2018 October 4

Abstract

Aperture synthesis arrays are commonly used in radio astronomy to take images of radio point sources, with the planned Square Kilometre Array (SKA) being the most common example. One approach to enhancing the quality of the images is to optimize an antenna array configuration in a possible SKA implementation. An ideal arrangement must ensure optimal configurations to capture a clear image by either decreasing the sidelobe level (SLL) in the l - m domain or increasing the sampled data in the spatial-frequency domain. In this paper a novel configuration is considered to optimize the array by considering all possible observation situations through the positions of the antenna array elements via a mathematical model that we call geometrical method (GM). To demonstrate its efficiency, the technique is applied to developing an optimal configuration for the elements of the Giant Metrewave Radio Telescope (GMRT). The effect of these changes, particularly in the forms of circular and spiral arrangements, is discussed. It is found that a spiral configuration results in fewer overlapping samples than the number of antennas placed along three arms of the GMRT with fewer than 11% and 27% overlapping samples in the snapshot and 6 hr tracking observations, respectively. Finally, the spiral configuration reduces the first SLL from -13.01 dB, using the arms of the current GMRT configuration, to -15.64 dB.

Key words: instrumentation: interferometers – telescopes

1. Introduction

One of the main activities in astronomy is measuring the angular positions of stars and other cosmic objects with adequate accuracy. This leads to the development of large and sensitive telescopes to detect small changes in celestial positions, which are an important step in the formation of the distance scale of the universe. Multiple telescopes or interferometer elements are often used together to form a synthesis array or interferometric array that can measure fine angular details in radio frequency range and capture an image of a radio point source in the sky. Subsequently, the spacing of the interferometer elements in the array plays an important role as this defines the sensitivity of the array to the spatial frequencies in the sky (Thompson et al. 2008).

The largest and most sensitive multi-radio telescope array will be the Square Kilometre Array (SKA) in the next decade. It involves the efforts of more than 10 countries. Although it will observe the blue sky and produce images with very high sensitivity, its image quality is still limited and affected by the sidelobe levels (SLLs; Hall 2007; El-makadema et al. 2014; Shahideh et al. 2014; Gie et al. 2016). On the other hand, it is shown that the value of unsampled points in the u - v coverage can be a standardized indication of the SLLs of the beam generated by an array system. Therefore, SLL suppression and uniform u - v plane coverage are important considerations in

developing an interferometer or synthesis array system (Thompson et al. 2008).

Optimization of an interferometric array then becomes the objective: an optimal array configuration must be able to capture a clear image of a radio point source by either decreasing the SLL in the l - m domain or increasing the sampled data in the spatial-frequency domain (which is referred to as u - v plane coverage; Shahideh et al. 2017). In other words, an optimized configuration attains the best possible u - v plane coverage in observations and the lowest SLL. Therefore, to optimize a synthesis array, the main properties of the array system that are used in astronomy, sensitivity, resolution, sampling accuracy, and signal-to-noise ratio, need to be considered in the development (Keto 1997).

To ensure high sensitivity, the number of array elements and the effective collecting area of each element (antenna) must be large. However, in practice, only a limited number of element antennas can be used because the cost of each element antenna is high (Thompson et al. 2008).

To ensure high resolution, element antennas, such as radio telescopes, have to be separated adequately, for example, by hundreds of kilometers (Thompson et al. 2008).

Sampling accuracy is another important parameter for the array, and it is shown that the uniform sampling comes with the least unsampled data. The signal-to-noise ratio of an interferometer observing a point source at the phase center of the image can be found to be (Thompson et al. 2008)

$$\frac{S}{N} = \frac{s}{n} \sqrt{n_d} \frac{\sum w_i}{\sqrt{\sum w_i^2}}, \quad (1)$$

where $\frac{s}{n}$, n_d , and w_i are the signal-to-noise ratio measured at a single sampling point, the number of data points in the sample, and the weights of the data, respectively.

To improve the sensitivity of the array, Keto (1997) proposed that the array elements be placed on a curved Y-shape instead of a Y shape for a better range of $u-v$ samples. Moreover, the samples in the $u-v$ plane should be circularly symmetric so that the array can have equal resolution in all directions for a high-resolution image. In particular, a high signal-to-noise ratio and the maximum resolution value can be obtained when the sampling is conducted uniformly in the Fourier domain within the boundary. Since an interferometric array discretely obtains samples from the Fourier components, incomplete sampling (or inaccurate sampling) and linear ridges indicate a non-uniform sampling (Keto 1997; Thompson et al. 2008).

Linear ridges of the $u-v$ plane coverage provide less object information in the snapshot observation or low-duration observations. Therefore, this drawback must be considered when designing an interferometric array. This scenario implies that an optimum configuration can provide an optimum solution in observations with one running algorithm or in a specific configuration. Thus, synthesis arrays for radio astronomy applications have been studied in depth and are well-documented over the past 60 years, and considerable work has been done so far.

A new method to reduce the SLL of an interferometric array with an element spacing much larger than the wavelength has been developed by Kogan (2000). This optimization method was designed to suppress the worst SLL of an interferometric array. The optimization algorithm was added to the task in the National Radio Astronomy Observatory astronomical image processing system (AIPS). Additionally, the algorithm has the advantages of considering some constraints, such as topography and minimum spacing between the array elements. Moreover, the algorithm is flexible for other additional constraints.

Woody (2001b) used different configurations such as pseudo-random and circular arrays, to investigate the SLL of the arrangements. The sidelobe distribution was followed by the theoretical distribution derived from Woody (2001a). It was found that the peak sidelobe as a function of the radial distance from the center of the point-spread function (PSF) is very useful for evaluating the PSF.

A new configuration of interferometer elements was suggested by Sodin & Kopilovich (2002). In this proposed method, elements were deployed on nodes of a regular hexagonal coordinate net. This caused no redundant coverage of a spatial-frequency domain. Additionally, this method provides the advantages of low SLL and high resolution. The authors also suggested that the geometry for constructing array configurations based on using cyclic difference sets might be useful for establishing radio interferometers of various wavelengths.

Notably, a hybrid array optimized for the HI emission surveys for an open-access radio telescope system, named the Australian SKA Pathfinder, was reported by Gupta et al. (2008). In it, 30 antennas were deployed around a circle of 2 km in diameter and 6 more antennas were placed within a Reuleaux triangle with a maximum separation of ~ 6 km. It achieves a good PSF at an angular resolution of $30''$ with SLLs of 2%–3% at 1.4 GHz. The particle swarm optimization (PSO) was applied to optimize the system with relatively short computation time (Bevelacqua & Balanis 2009).

Mort et al. (2016) provided some options for station designs for the Square Kilometre Array's Low Frequency instrument (SKA-LOW) and proposed that the dynamic logical regrouping of the antennas could improve the shape and sidelobe cancellation of the station beams.

To achieve the most appropriate $u-v$ plane sampling for astronomical imaging, Karastergiou et al. (2006) presented a low-density system based on the ideas of Keto (1997) and Boone (2001, 2002). A Bessel decomposition-based algorithm was proposed. The algorithm is sensitive to large-scale over- and underdensities in the $u-v$ plane (Beardsley et al. 2012). A new theory of compressed sensing was introduced with the use of the orthogonal matching technique to compensate for incomplete sampling of the Fourier plane (Fannjiang 2013). To obtain the optimum solutions for the $u-v$ density distribution and the PSF for the SKA, genetic optimization was applied (Beardsley et al. 2012; Fannjiang 2013; Gauci et al. 2013). Unfortunately, the above-mentioned work did not take the SLL suppression into account, which is important for a clear image of a radio point source.

Even though various techniques have been developed for the interferometric array, only few of them have considered all desired requirements while optimizing the array system (see Shahideh et al. 2017). Moreover, in some of the works, the results are presented in figures and displayed visually without using any equations to precisely compare different configurations. However, a method of presentation must be chosen to carefully weigh the advantages and disadvantages of different methods. In this paper, a new method, which is called geometrical method (GM), quantitatively assesses the effect of the array configuration on imaging performance, introducing the overlapping samples and unsampled cells through new and simple equations as prime figures of merit. In addition, it is problematic to rank configurations in terms of their $u-v$ coverage by simple visual inspection. The GM identifies the most uniform $u-v$ coverage.

This paper reports on the results of research conducted for the Giant Metrewave Radio Telescope (GMRT) and can be used for the upcoming SKA telescope and precursors on the shapes of interferometers constructed with a design based on either fixed layout, spiral or mounted on a rail track. Since the configurations follow some geometric formulas, the proposed method ranks the best configuration with low computational cost and complexity.

These reasons are novel about the configuration designs, which are easy, fast, adaptive, and provide deterministic results even when the array has an approximate shape because of some constraints, unlike the more randomized layouts developed in other recent layout optimizations, such as genetic algorithms or PSOs to optimize arrays for specific figures of merit.

Different configurations are presented to prove the efficiency of our method in designing an array with typical open- and closed-armed configurations such as a Y or circular configuration. This is done by changing the antenna coordinates of the representative existing design to obtain optimum arrays.

This paper is organized in the following manner: Section 2 presents the current situation, and Section 3 proposes our technique and the results. Sections 4 and 5 cover the discussions and conclusion.

2. Method

An optimized configuration must provide high sensitivity to a point source, angular resolution, signal-to-noise ratio, and

sampling accuracy, which can be used in either the snapshot or hour-tracking observation. In a designed array situation where the number of array elements, effective collecting area, and maximum element separation are defined to satisfy the common properties of the array system, uniform sampling will be of interest.

Designing the appropriate spatial layout of the antennas in a correlator array is essentially an optimal sampling problem. The imaging qualities of an interferometric telescope are dictated by the characteristics of the synthesized beam, which depend mostly on the localization of the antennas comprising the telescope and the coordinates of the astronomical source during an observation. However, the location of the antennas should allow for optimal performance in all the significant requirements such as the maximum $u-v$ plan and low SLL synthesize beam. In general, the samples on the $u-v$ plane should be distributed with a large enough distance to ensure that all parts of the $u-v$ plane are sampled, and the SLL should be as low as possible (Karastergiou et al. 2006). For instance, the $u-v$ plane of the SKA configuration must meet different fundamental scientific requirements such as good snapshots and long baselines for milliarcsecond imaging. The antennas must provide good $u-v$ coverage to satisfy these requirements (Lal et al. 2010). The SKA will be a facility approximately one order of magnitude more sensitive than the Square Kilometre Array Phase 1 (SKA1) with a maximum baseline as large as 3000 km (see Braun et al. 2015; Torchinsky et al. 2017). An optimal configuration depends on an optimized $u-v$ plane by suppressing SLLs. To satisfy this issue effectively, this study introduces two prime figures of merit, overlapping samples and unsampled cells, to ensure uniform sampling in the $u-v$ plane. This will give equal sensitivity to all spatial scales sampled by an interferometer.

Therefore, this paper starts with a configuration whose the $u-v$ coverage provides a uniform distribution of sampling points within a circular boundary, and then investigates concentric circles and spiral shapes to meet the desired requirements.

Generally, one well-known galaxy shape is a spiral. The first types of galaxies that would be recalled are shown in Figure 1. These configurations can be thought of as some overlapping circles in a specific area. The antennas are deployed along the chords of each circle in a shape consisting of several circles (see Figures 1(a)–(b)) or along the chords of circles that their radii increase from the central circle to the boundary circle (see Figure 1(c)). Therefore, the next investigated configuration is a spiral shape based on the reasons below:

1. They consist of several circles and might have the advantage of circular configurations.
2. They have the shape of most known galaxies and are curved.

Specifically, the effect of these curved configurations on the $u-v$ plane coverage and SLL is considered instead of working on computation-intensive configurations resulting from known algorithms, such as a genetic algorithm. It should be taken into account that there are several previous investigations on different types of curved shapes (e.g., Ghosh et al. 2012; Sengupta et al. 2012; Shahideh et al. 2013), but only few of them have been conducted to optimize the configuration of an interferometric array, which needs to consider some desired requirements. Moreover, there are many SKA studies on different configurations including spiral configurations (see

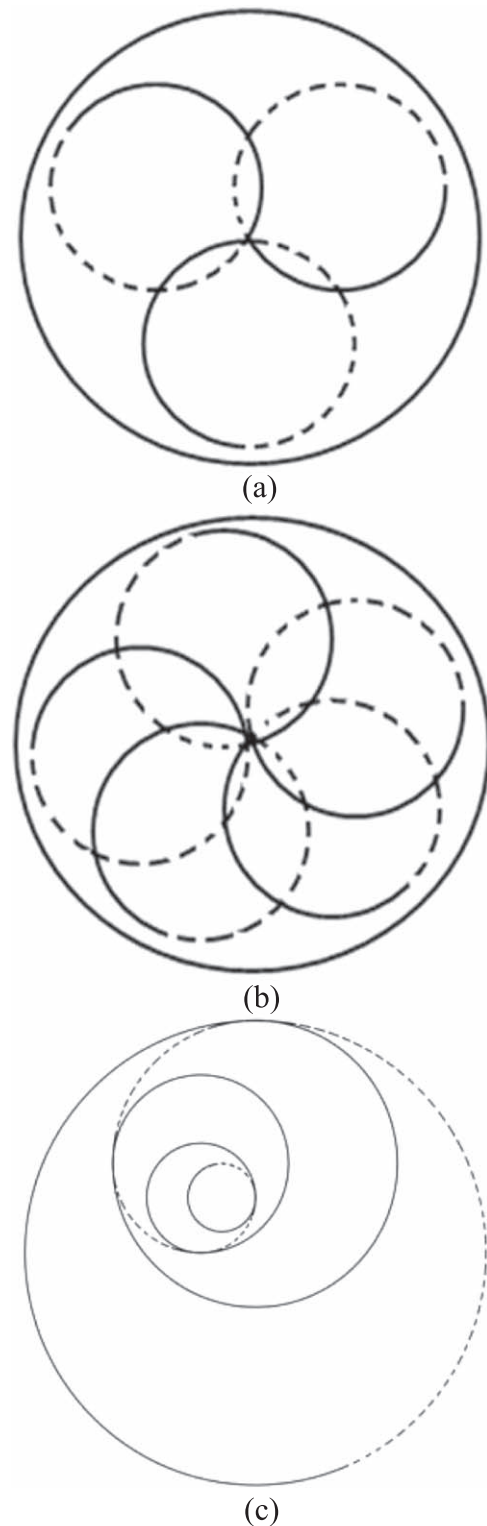


Figure 1. Spiral shape consisting of (a) three and (b) five overlapping circles in a specific area and (c) a spiral shape consisting of various circles with different radii.

Grainge 2014), but none of them explained and compared the effect of changing the curvature and increasing the number of arms or circles on the $u-v$ plane and SLL while the number of antennas remained the same.

The GM uses the optimization of the array configuration problem with various changes of coordinates in a specific area

with the GMRT arms as an illustrative example. The GMRT is located 80 km north of Pune, India ($19^{\circ} 6' N 74^{\circ} 3' E$). It is an open-end configuration resembling a Y shape, and has 30 parabolic dish antennas that are 45 m in diameter each. Basically, the antennas are located in the GMRT based on several factors. The two main factors are (a) the aim to obtain the maximum coverage in the spatial-frequency domain; and (b) the size of the sources to be studied. Particularly, long baselines are adopted for small sources, whereas short baselines are used for extended sources. Given that the antenna locations in the GMRT are fixed, both compact and extended arrays are employed to meet the desired requirements (Swarup et al. 1991).

Therefore, a total of 14 antennas are located randomly in an area of $\sim 1 \text{ km}^2$ in this array as a compact array. The remaining 16 dishes are extended along the three arms with the largest baseline of $\sim 25 \text{ km}$ as an extended array. The operating frequency ranges of the GMRT are $\sim 50, 151, 232, 327, 610,$ and 1420 MHz , which are metered wavelengths (Kapahi & Ananthkrishnan 1995).

To gain a good insight into such an analysis, the existing coordinates of 16 antennas of the GMRT spread out along three arms of the Y shape were used to investigate the effect of different configurations of arms on sampling the u - v planes and SLL carefully. They were then replaced by placing these 16 antennas in configurations of two concentric circles (2-circle), three concentric circles (3-circle), three spiral arms (3-arm), five spiral arms (5-arm), and a spiral (the new proposed configuration).

The GM first uses geometric formulas to outline the configurations. For instance, it uses the formula of a logarithmic spiral for the spiral layout. Second, it finds the latitudes and longitudes of the antennas and converts them into the rectangular coordinates according to the formula below:

$$\begin{aligned} X &= R \times \sin \theta \times \cos \varphi \\ Y &= R \times \sin \theta \times \sin \varphi \\ Z &= R \times \cos \theta, \end{aligned} \quad (2)$$

where θ , φ , and R are latitude, longitude, and radial distance, respectively.

Then, discrete two-dimensional Fourier transform is used in this paper to synthesize an image. Therefore, in this study the u - v plane achieved by different configurations is gridded using the equation

$$N_{\text{grid}} = \sqrt{\left(\frac{A_t}{A}\right)} \times (\text{nosmp}). \quad (3)$$

Here nosmp is the number of samples in the snapshot or hour-tracking observation, A_t is the total desired area, A is the area covered by the current configuration, and N_{grid} is the number of gridded cells.

The dimension of each cell is $\Delta u \times \Delta v$, and the following equations are used to calculate the values of the Δu and Δv :

$$\Delta u = \frac{u_{\text{max}} - u_{\text{min}}}{N_{\text{grid}}} \quad (4)$$

$$\Delta v = \frac{v_{\text{max}} - v_{\text{min}}}{N_{\text{grid}}}, \quad (5)$$

where Δu , Δv , u_{max} , u_{min} , v_{max} , v_{min} , and N_{grid} are the dimension of the cell in the u direction, the dimension of the cell in the

v direction, the maximum value of u in the spatial-frequency domain, the minimum value of u in the spatial-frequency domain, the maximum value of v in the spatial-frequency domain, the minimum value of v in the spatial-frequency domain, and the number of gridded cells as defined in Equation (3), respectively.

Then, the number of samples in each cell is calculated. If a cell has more than one point sample of a spatial frequency, it means that this cell has overlapping samples. In order to have a good-quality sky image, the samples should be distributed smoothly, and each cell should preferably contain one sample. The overlapping samples of each cell are calculated using the equation

$$ol_i = \text{cell}_i - 1, \quad (6)$$

where ol_i and cell_i are the number of overlapping samples in the i th cell and the number of samples in the i th cell, respectively.

Cells without any samples show that the configuration was not able to cover that area, and these are defined as unsampled cells in this work.

The mean SLL can be calculated using the following equation:

$$\text{mean SLL} = \text{mean}(\text{first SLL} + \text{second SLL} + \text{third SLL}), \quad (7)$$

here first SLL, second SLL, and third SLL are the peak values of the first, second, and third SLL, respectively, generated by the configuration.

Finally, the GM is able to rank the different configurations after calculating the overlapping samples, unsampled cells, and SLL.

3. Results

To compare all configurations with a high degree of precision, the configurations were simulated in AIPS, using a Gaussian source, and then SLLs were calculated. The first three SLLs at a 90° cut from the source, the mean value of the first three SLLs, and the worst SLL were investigated. It should be noted that the worst SLL, defined as peak SLL, occurs in any direction other than 90° .

The horizontal and vertical axes in the u - v plane indicate $u \times \lambda \text{ km}$ and $v \times \lambda \text{ km}$, respectively. In general, the duration of the tracking observation is $2h$ (where h is between 0 and 12 hr, unit: hours) and the time interval between two samples is (Δh). The value of each instant hour angle will be in the range of $(-h)\pi/12$ ($h)\pi/12$) in radians.

The antennas are located in the same area as those of the GMRT. The source decl. for all configurations is the same (decl. = 45°). The spiral configuration follows the formula of a logarithmic spiral. The coordinates of the antennas were calculated using geometric formulas.

Snapshot plots show the Fourier components that are measured instantaneously by different configurations ($H = 0^h$). The duration of the tracking observation is $h = 6 \text{ hr}$ (where h is between -3 and 3 hr , unit: hours) and the time interval between two samples is $\Delta h = 10 \text{ minutes}$.

Figure 2 demonstrates the different configurations of GMRT, the GMRT compact array, the GMRT without a compact array, 2-circle, 3-circle, 3-arm, 5-arm, and spiral.

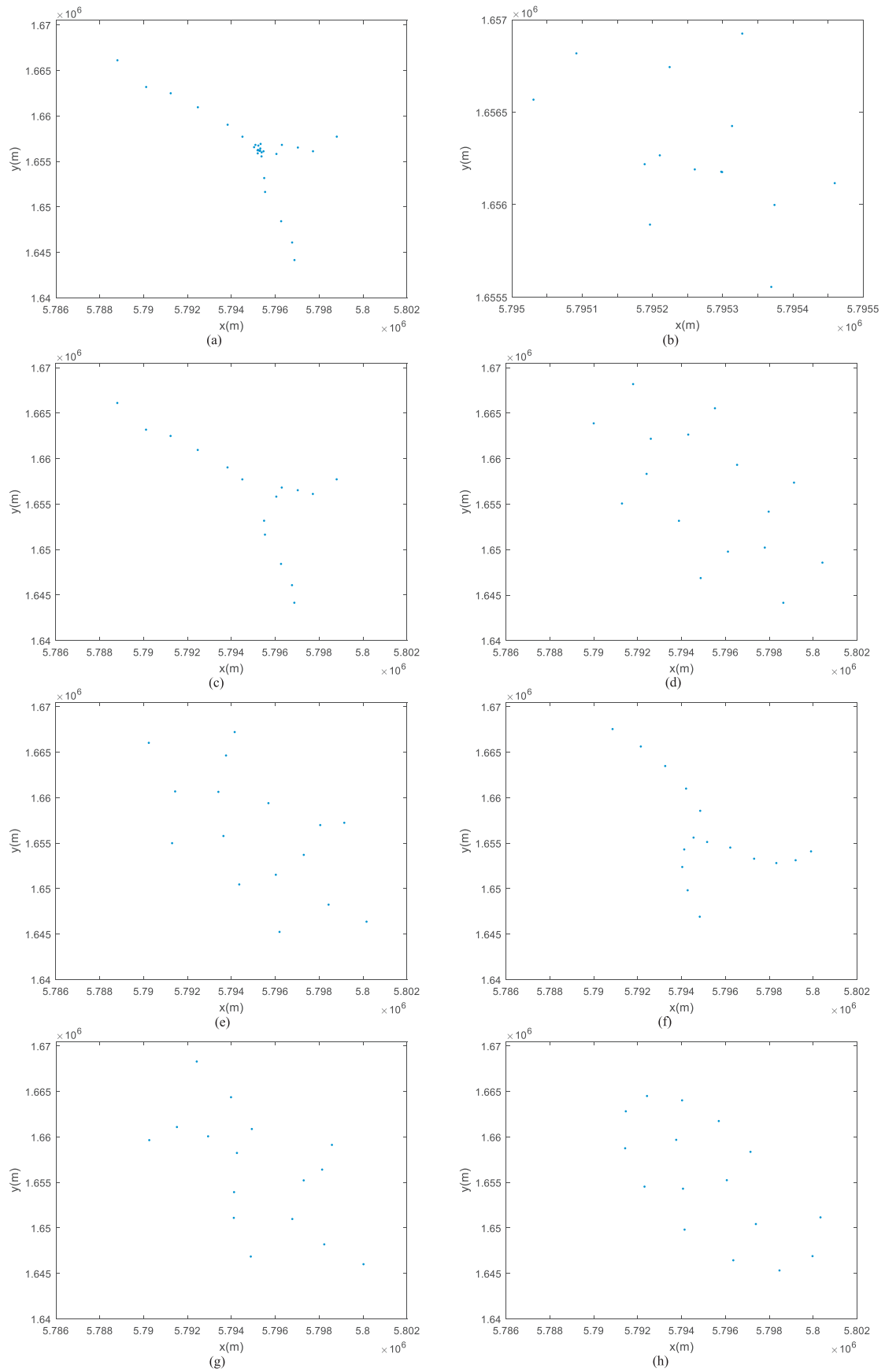


Figure 2. Configuration of (a) the GMRT antennas (approximately in a Y shape), (b) 14 GMRT antennas in a square of $\sim 1 \text{ km}^2$, (c) the GMRT without a compact array, (d) 2-circle, (e) 3-circle, (f) 3-arm spiral, (g) 5-arm spiral, and (h) a spiral.

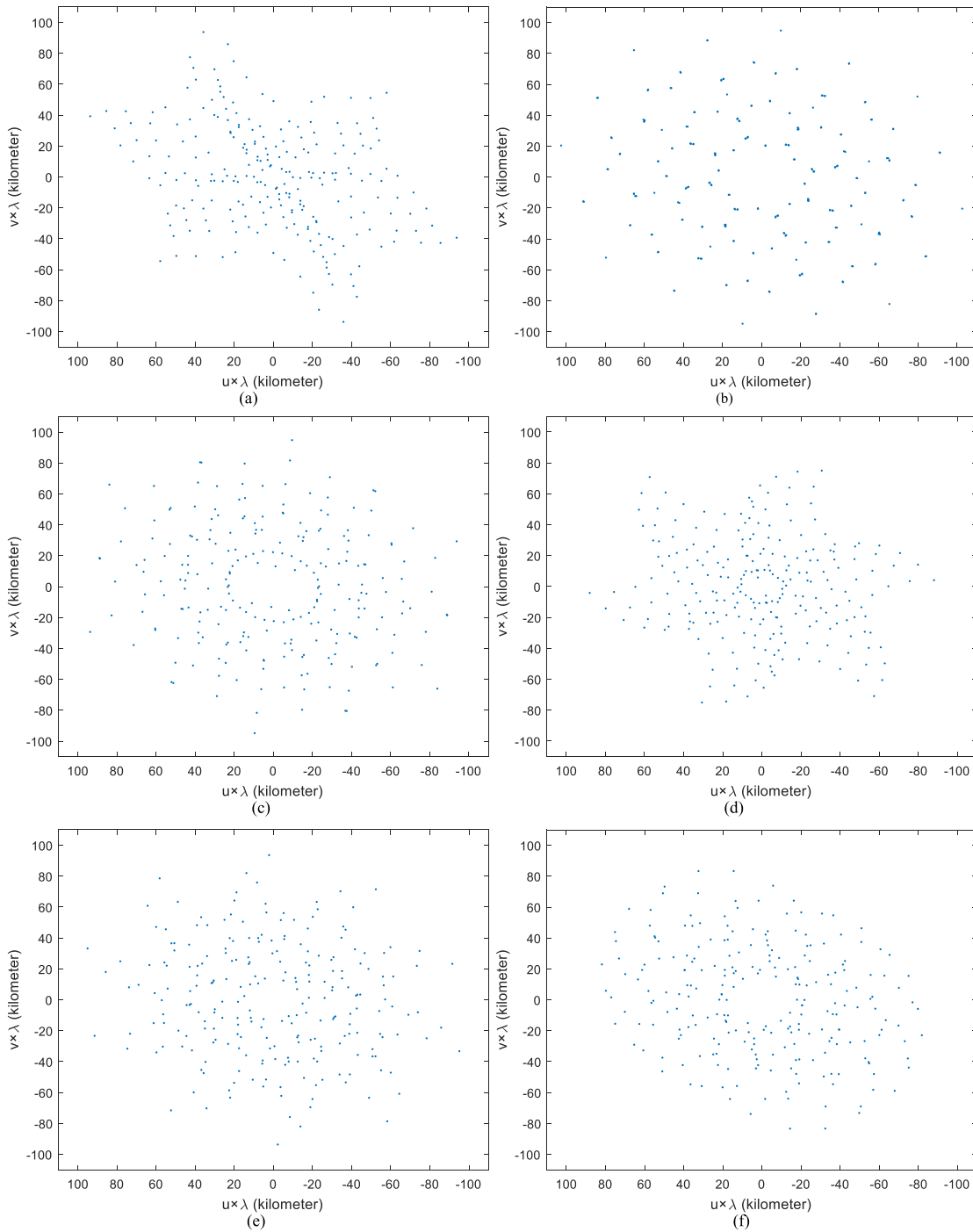


Figure 3. Spatial-frequency coverage in the snapshot observation of (a) the GMRT without compact array, (b) 2-circle, (c) 3-circle, (d) 3-arm spiral, (e) 5-arm spiral, and (f) a spiral.

To grid the $u-v$ plane, Equations (3)–(5) are used for the configuration of 16 antennas deployed along three arms of the GMRT, and the same achieved $N_{\text{grid}s}$ in either observation were used for all the configurations.

The resultant $u-v$ coverage planes of the snapshot and 6 hr tracking observations are shown in Figures 3 and 4, respectively.

The calculated overlapping samples and unsampled cells in the snapshot and 6 hr tracking observations are shown in Table 1.

Figures 2(a)–(b) show the configuration of the GMRT and its compact array. The 16 antennas of the GMRT without its compact array and the calculated $u-v$ plane coverages in the snapshot and 6 hr tracking observations are indicated in Figures 2(c), 3(a), and 4(a), respectively.

As demonstrated in Table 1, the current configuration of the GMRT mostly works better than an exact Y-shape. The overlapping samples in the snapshot and 6 hr tracking observations are 20% and 35.6% for the Y shape, and 17.5% and 34.7% for the GMRT. The unsampled cells are 83.8% and

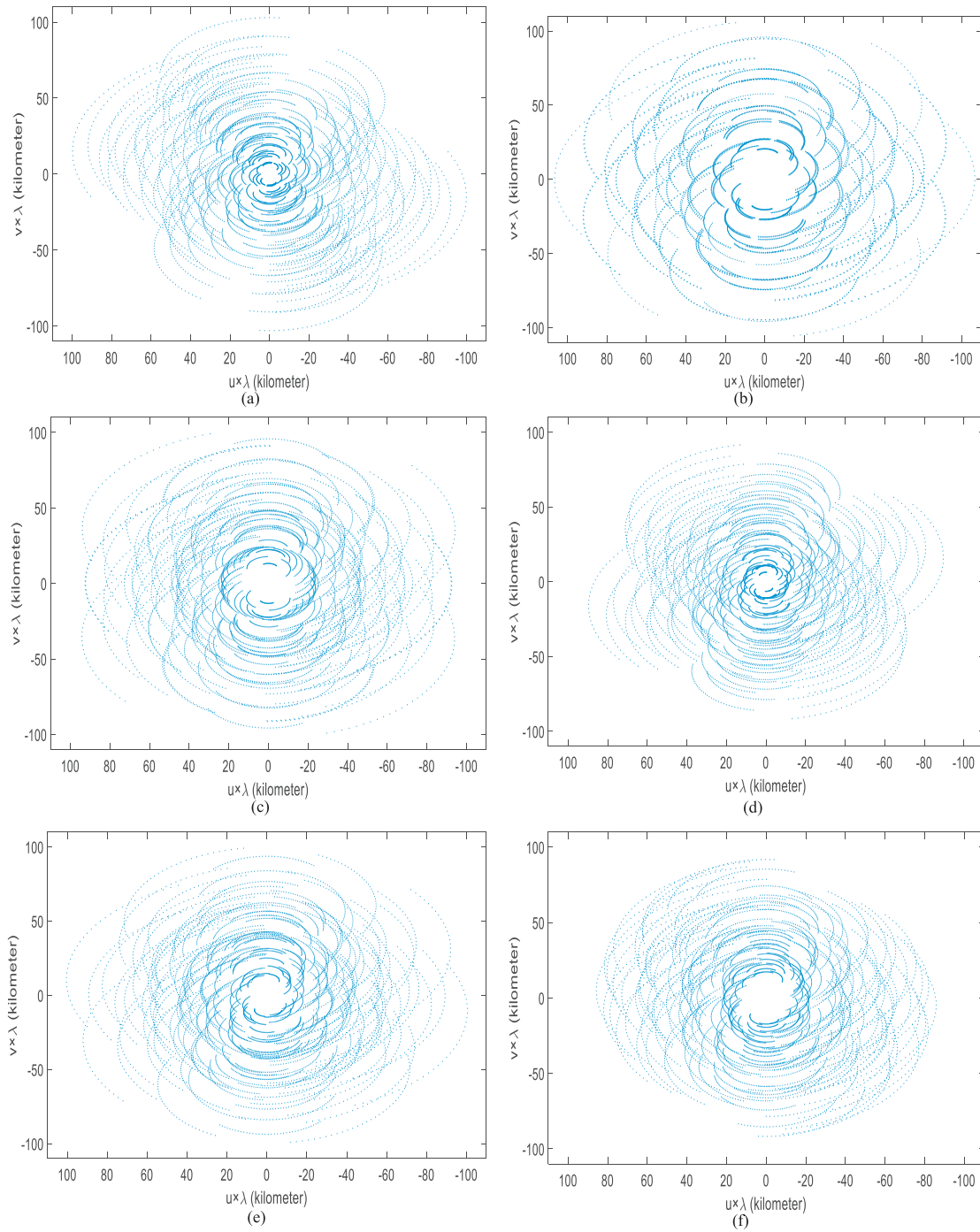


Figure 4. Spatial-frequency coverage in 6 hr tracking observation of (a) the GMRT without compact array, (b) 2-circle, (c) 3-circle, (d) 3-arm spiral, (e) 5-arm spiral, and (f) spiral.

82.2% for the Y shape, and 79.9% and 82.5% for the GMRT. The current GMRT configuration performs better than an exact Y-shape array, which might be due to the slight curvatures of the GMRT arms.

A closed-arm configuration such as a circle is used in radio astronomy. In this paper, a configuration of two- concentric circles (see Figure 2(d)) was designed before a configuration with three concentric circles was considered. The arrangement consists of two concentric circles each consisting of eight antennas around each circle. It is shown in Figure 3(b) that in the snapshot, the linear ridges are smooth, but there are many overlapping samples. There many gaps in hour-tracking and

snapshot observations (Figures 3(b) and 4(b)). It is depicted in Figure 3(b) in the snapshot observation that the 2-circle gives a smoother boundary than the GMRT. Although the configuration of 2-circle smoothens the linear ridges, it has very poor $u-v$ coverage in both observations. Table 1 shows that the overlapping samples of this configuration are very high for both observations as compared to the GMRT arms, and it is valued at 51.7% (in snapshot) and 50.0% (in 6 hr tracking) for the 2-circle, and 17.5% (in snapshot) and 34.7% (in 6 hr tracking) for the GMRT. The GMRT arms sample the Fourier space of the image better than the 2-circle, even though the Fourier domain within the boundary in the 2-circle is sampled

Table 1
Comparison of the GMRT and Different Configurations

Configuration	Overlapping Samples% (Snapshot)	Overlapping Samples% (Hour Tracking)	Unsampled Cells% (Snapshot)	Unsampled Cells% (Hour Tracking)
Y shape	20.0	35.6	83.8	82.2
GMRT	17.5	34.7	79.9	82.5
2-circle	51.7	50	87.5	86.1
3-circle	15.8	29.1	78.6	80.5
3-arm	8.3	31.6	78.0	81.1
5-arm	16.7	31.1	79.0	81.0
Spiral	10.8	26.6	78.2	80.3

Note. 6 hr is used in the hour-tracking synthesizer.

more uniformly. The calculated unsampled cells in the snapshot and the hour-tracking observations are 87.5% and 86.1% for the 2-circle, and 79.9% and 82.5% of the GMRT, respectively.

This configuration has a good boundary for short-duration observations; therefore, we were motivated to increase the number of circles, while the number of antennas remained the same. The 3-circle configuration consists of three circles consisting of two circles of five and one circle of eight antennas, respectively. This configuration and its related $u-v$ coverage planes in the snapshot and 6 hr tracking observations are shown in Figures 2(e), 3(c), and 4(c) respectively.

As shown in Figures 3(c) and 4(c) and indicated in Table 1, the 3-circle gives more information due to the greater number of samples in the $u-v$ plane and fewer overlapping samples than the 2-circle. Table 1 indicates that the $u-v$ coverage in 6 hr tracking of the 3-circle gives fewer overlapping samples than the 2-circle because of the greater number of samples in the $u-v$ plane than the 2-circle. The overlapping samples are valued at 15.8% and 29.1% in the snapshot and 6 hr tracking observations, respectively. The results of unsampled cells (78.6% and 80.5% in the snapshot and 6 hr tracking observations, respectively) show that the 3-circle samples the Fourier space of the image better than the 2-circle and the GMRT.

Another way to optimize an array of antennas is to curve the arms of the Y shape. Some overlapping circles in a specific area are used by deploying the antennas along the chords. Figures 1(a) and (b) depict three and five overlapping circles in the same area as where the GMRT antennas are deployed.

Another configuration that was done before a five-arm spiral is the three-arm spiral shown in Figure 3(f). To design a three-arm spiral, three arms of 16 antennas are spread out along three arms of a spiral in the same region of the GMRT. These arms are equi-angular (120°) and are spaced and spread out up to 12.5 km.

The values of overlapping samples in the snapshot and 6 hr tracking observations are 8.3% and 31.6%, respectively. Furthermore, there are fewer unsampled cells in the snapshot observation than in the 3-circle (78.0%). Although the 3-arm works better than the 3-circle in terms of overlapping samples in the snapshot and unsampled cells in the 6 hr tracking observation, the linear ridges of the 3-circle, overlapping samples, and unsampled cells in the 6 hr tracking are better than in the three-arm configuration.

Because increasing the number of circles in concentric circles had a significant effect on the results, we were motivated to increase the number of arms in the spiral shape while the number of antennas remained the same.

To design a five-arm system, 16 antennas are spread out along five spiral arms of 12 antennas along four arms and 4 antennas along one arm. The angular distance between each two arms is 72° and the antennas are spread out extending up to 12.5 km.

The $u-v$ coverage in the 6 hr tracking observation has samples with 31.1% overlapping samples, so this parameter shows better coverage than in the three-arm configuration (see Figure 4(e) and Table 1). Its value of overlapping samples in the snapshot (16.7%) is lower than the GMRT and 2-circles. However, the five-arm spiral works better than the GMRT arms for both observations. The unsampled-cells parameter is valued at 79% and 81% in the snapshot and 6 hr tracking observations, respectively. The results show that the five-arm spiral works better than the three-arm spiral in the 6 hr tracking observation.

The results in Table 1 show that increasing the number of arms improves the 6 hr tracking observation. On the other hand, increasing the number of circles is more effective for results than increasing the number of arms in terms of the $u-v$ coverage. The next configuration we investigate below is the spiral.

To smoothen out linear ridges in the spatial-frequency domain, the five-arm spiral can be replaced by a shape consisting of several circles with increasing radii from the center to the boundary as a new configuration in this study (see Figure 1(c)). This suggests that antennas can be placed in a spiral geometry. Figure 2(h) shows that there are one and a half curves around the first antenna at the center. The length of the arm spread extends to 12.5 km.

The distribution of samples is very good (see snapshot in Figure 3(f)). The ridges are very smooth in the snapshot. Observations of the snapshot (with overlapping samples of 10.8%) in Figure 3(f) and the 6 hr synthesis (with overlapping samples of 26.6%) in Figure 4(f) illustrate a very good coverage in the $u-v$ plane. The values of unsampled cells are 78.2% and 80.3% in the snapshot and 6 hr tracking observations, respectively.

In order to satisfy the requirements of the observations, the SLLs from the synthesis beam or the PSF resulting from different configurations simulated in AIPS have also been investigated (Table 2).

The calculated SLLs in Table 2 show that the first SLL achieved with 16 antennas spread out along the three arms of the GMRT is -13.01 dB and the mean value of the first three SLLs is -11.67 dB with the peak SLL of -9.96 dB. The calculated SLLs in Table 2 illustrate that the first SLL, the mean values of the first three SLLs (mean SLL), and the peak SLL are valued at -13.17 dB, -10.71 dB, and -7.23 dB for

Table 2
Comparison of the GMRT SLL and Different Configurations of SLL

Configuration	First SLL (dB) (Hour Tracking)	Mean SLL (dB) (Hour Tracking)	Peak SLL (dB) (Hour Tracking)
GMRT	-13.01	-11.67	-09.96
2-circle	-06.25	-09.35	-06.54
3-circle	-13.17	-10.71	-07.23
3-arm	-14.46	-15.67	-11.12
5-arm	-17.57	-17.68	-11.64
Spiral	-15.64	-14.74	-11.27

Note. 6 hr is used in the hour-tracking synthesis.

the 3-circle, respectively, which shows a better performance than the 2-circle in terms of suppressing SLL (i.e., -6.25 dB, -9.35 dB, and -6.54 dB, respectively). The GMRT arms have a lower SLL than the 3-circle, excluding the first SLL. Therefore, results in Tables 1 and 2 of the $u-v$ coverage and SLLs show that increasing the number of circles, but not the number of antennas, which remains the same, provides better results.

The values of the first SLL, mean SLL, and the peak SLL of the 3-arm (-14.46 dB, -15.67 dB, and -11.12 dB, respectively) and the 5-arm (-17.57 dB, -17.68 dB, and -11.64 dB, respectively) indicate that n -arm spiral configurations provide lower SLL than a Y shape, in addition to the fact that increasing the number of the arms of the spiral with the same number of antennas suppresses the levels of SLLs. Results from the $u-v$ plane coverage and SLLs have shown that by increasing the number of arms without changing the number of antennas, better results are obtained in most cases.

Finally, the spiral configuration provides lower values of the first SLL, mean SLL, and peak SLL (-15.64 dB, -14.74 dB, and -11.27 dB, respectively) than a Y shape and concentric circles. This suggests that the spiral configuration meets the desired requirements of good $u-v$ coverage with low SLLs.

Since increasing the number of circles affects the SLL, concentric configurations with more circles consisting of several rings distribute the antennas in the same area more smoothly than a smaller number of the circle configuration. Consequently, increasing the number of the arms decreases the SLL more effectively than increasing the number of concentric circles. This means that a curving open-armed configuration works better than the closed-arm configuration in terms of SLL. Furthermore, spiral configurations suppress the SLLs better than the GMRT and concentric circle configurations discussed in this study, while spiral configurations try to distribute the $u-v$ samples more smoothly with antennas covering the area better.

4. Discussion

Designing an interferometric array is the main objective of this study, which considers all possible performance metrics, such as the lowest SLL in the angular domain (i.e., the $l-m$ domain), and increases the distributed data ratio on the $u-v$ plane to observe the radio frequency range and a maximum coverage in the spatial-frequency domain (i.e., the $u-v$ domain). Therefore, this paper attempts to investigate a solution to optimize such an array by considering all possible performance metrics.

In this paper, a straightforward method, the GM, is developed to account for the main properties of the array system through different parameters. Compared to the different methods, the GM provides an easier and also more flexible technique to optimize the array by regarding all possible observation situations through the positions of the antennas via specific mathematical models. Whereas the method is not non-deterministic and random, it has the ability to provide a configuration that can be useful for arrays that are mounted on rail and for a fixed array layout. The proposed arrays can be used when antennas are mounted on a rail due their proficiency and easy design. They do not need many computations and algorithms. Therefore, it is easy, adaptable, not time-consuming, and always converges to reasonable results, unlike other randomized algorithms. On the other hand, when the array should be fixed like the GMRT, this method would meet almost the desired requirements for astronomy applications. Moreover, the method can also provide good results if the position of some antennas in the array layout should be changed due to some constraints like the GMRT (the configuration of the GMRT was supposed to be an exact Y shape, but it is only approximately Y-shaped due to some constraints).

The GM introduces new equations to achieve these essential parameters that can be used to weigh the merit and demerit of different methods. Different configurations (open- and closed-arm arrays) are discussed. The GM proposes some advantages for practical array designs. First, the method is easy to implement to meet the desired requirements (main properties of the array system) instead of working on computation-intensive configurations resulting from known algorithms such as a genetic algorithm. Second, the GM is able to work on a large number of antennas, with different sizes of telescopes. Finally, the method is adaptive, quick, and very flexible to different geographical constraints. This proposed method can be applied to a system such as the SKA to achieve improvements and allows the scientists to observe the sky with an enhanced image or the GMRT as an existing correlator array antenna for the expansion of the array to obtain a higher resolution.

This paper proposes an idea that leads to optimum solutions for astronomy applications and suggests that it may be applicable to much larger arrays, such as the SKA. Not only did we show that curving the arms in a spiral could smoothen the linear ridges in a snapshot, but it also decreases SLLs (see results of 3-arm and GMRT configurations). Moreover, increasing the number of arms in the spiral or increasing the number of circles in concentric circle configurations decreases the SLL, as was shown in the literature we cited in the Introduction. The following new results were obtained and are reported in this paper:

- (1) Curving open-arm configurations perform better than closed-arm configurations in terms of SLL.
- (2) Increasing the number of circles or the number of arms provides better results in terms of suppressing SLL.
- (3) Increasing the number of circles provides better results in terms of the $u-v$ coverage.
- (4) Using any spiral configuration meets the desired requirements for astronomy applications, such as decreased overlapping data on the $u-v$ plane in both the snapshot and hour-tracking observations, low SLL, and smooth boundary especially in the snapshot observations.

- (5) The spiral configuration distributes the samples more effectively than the GMRT, n -arm, and n -circle configurations.

In terms of the properties of the GM, it is also found that

- (1) This method is adaptive, quick, and easy to implement in order to achieve the desired requirements.
- (2) There is no need to run an algorithm separately to achieve an optimized configuration to increase the number of samples in a snapshot and to suppress the SLL.
- (3) To quickly adapt the observing strategy for a given array on the track, this method provides fast and reliable results.
- (4) For a fixed array, the GM is suggested to be used as the antennas are not movable and the method yields the desired requirements in the most important scientific aspects.

This work aimed at investigating the effect of different configurations of arms on the u - v plane and SLL and at finding a configuration that is able to meet the most desired requirements. Furthermore, as future work, the optimized shape of the spiral can be investigated by changing the spacing of antennas along the curve, i.e., the curvature of the spiral, by combining other configurations (e.g., mixing spiral with circle), and applying known algorithms such as the GA to find an optimized spacing of antennas in the spiral configuration array. Different important types of two-dimensional spirals such as an Archimedean spiral and a Fermat spiral can also be investigated as future work. It should be noted that in order to gain a higher precision, some changes such as the spacing of antennas in each arm or the curvature of arms are needed.

This method is also suitable if the antennas are mounted on a rail track, and one can change the configuration depending on the nature of the astronomical observations. Since the configurations simply follow some geometric formulas, the GM is deterministic, does not require heavy computations, and does not consume much time.

5. Conclusion

The GM is used to optimize the array by considering all possible observation conditions. Various configurations are presented to render the effectiveness of the method in designing a correlator wearable with typical open-terminated and closed configurations. The said output can be attained by changing the optimum arrays that outperform habitant arrays and represent existing designs. An interferometer with a curved shape of constant width is proposed to provide improved sensitivity by obtaining a better range of u - v samples. High reliability, sensitivity, signal-to-noise ratio, and distributed data ratio on the u - v plane to observe the radio frequency range are obtained because of the few overlapping samples and suitably distributed samples.

In order to simulate the hour-tracking observations of a radio source with the same time duration and source decl., the Earth rotation effect is considered in this paper. The results show that spiral configurations offer very good results in both the aspects of the u - v plane and the side lobes. It is found that a spiral configuration results in fewer overlapping samples in both the snapshot and hour-tracking observations than one in which the antennas are placed along three arms of the GMRT, with less than 11% and 27% of overlapping samples in the snapshot and hour-tracking observations, respectively. Furthermore, the configuration of the spiral is able to show the fewest unsampled cells in the gridded u - v coverage in the hour-tracking observation (80.3%)

when compared to other configurations discussed in this study. Finally, the spiral configuration reduces the first sidelobe from -13.01 dB, using the arms of the current GMRT configuration, to -15.64 dB, and the five-arm spiral configuration has the lowest values of the first SLL, mean value of the first three SLLs, and the peak SLL of -17.57 dB, -17.68 dB and -11.64 dB, respectively.

In summary, the novelty of the GM is that it retains simple, fast, adaptive, and deterministic results, unlike the more randomized layouts developed in other recent layout optimizations, such as the GA and PSO, which have been used to optimize arrays for specific figures of merit.

This work was supported by the NSERC's (Natural Sciences and Engineering Research Council) CREATE (Collaborative Research and Training Experience) Program entitled ASPIRE (Advanced Science in Photonics and Innovative Research in Engineering) of Canada and by European Regional Development Fund in the IT4Innovations National Supercomputing Center—Path to Exascale Project, project number CZ:02:1:01=0:0=0:0=16_013=0001791 within the Operational Programme Research, Development and Education.

ORCID iDs

Shahideh Kiehadrouinezhad  <https://orcid.org/0000-0002-2025-0088>

References

- Beardsley, A. P., Hazelton, B. J., Morales, M. F., et al. 2012, *MNRAS*, **425**, 1781
- Bevelacqua, P. J., & Balanis, C. A. 2009, *ITAP*, **57**, 1285
- Boone, F. 2001, *A&A*, **377**, 368
- Boone, F. 2002, *A&A*, **386**, 1160
- Braun, R., Bourke, T., Green, J. A., Keane, E., & Wagg, J. 2015, in *Advancing Astrophysics with the Square Kilometre Array*, Proc. AASKA14 (Trieste: SISSA), 174
- El-makadema, A., Rashid, L., & Brown, A. K. 2014, *ITAP*, **62**, 1673
- Fannjiang, C. 2013, *A&A*, **559**, A73
- Gauci, A., Adami, K. Z., Abela, J., & Cohanin, B. E. 2013, *MNRAS*, **431**, 322
- Ghosh, P., Banerjee, J., Das, S., & Chowdhury, S. S. 2012, *Progress In Electromagnetics Research (PIER)*, **43**, 333
- Gie, H. T., et al. 2016, *Proc. SPIE*, 9906, 990660
- Grainge, K. 2014, arXiv:1404.6184
- Gupta, N., Johnston, S., Feain, I., & Cornwell, T. 2008, ATNF SKA Memo Series (Australia Telescope National Facility, CSIRO), 016
- Hall, P. J. 2007, An SKA Engineering Overview Memo, 91, <https://pdfs.semanticscholar.org/4e5b/058416f12f278d4cebb127606e230396c492.pdf>
- Kapahi, V. K., & Ananthakrishnan, S. 1995, *BASI*, **23**, 265
- Karastergiou, A., Neri, R., & Gurwell, M. A. 2006, *ApJS*, **164**, 552
- Keto, E. 1997, *ApJ*, **475**, 843
- Kogan, L. 2000, *ITAP*, **48**, 1075
- Lal, D. V., Lobanov, A. P., & Jiménez-Monferrer, S. 2010, arXiv:1001.1477
- Mort, B., Dulwich, F., Razavi-Ghods, N., Acedo, E. de L., & Grainge, K. 2016, *MNRAS*, **465**, 3680
- Sengupta, A., Chakraborti, T., Konar, A., & Nagar, A. K. 2012, *Progress In Electromagnetics Research (PIER)*, **42**, 363
- Shahideh, K., Daniela, V., Michael, C., Noordin, N. K., & Shahabi, A. 2017, *AJ*, **154**, 167
- Shahideh, K., Kyun, Ng. C., & Noordin, N. K. 2013, in *IEEE Space Science and Communication (IconSpace) Conf.* (New York: IEEE), 39, doi:10.1109/IconSpace.2013.6599429
- Shahideh, K., Noordin, N. K., Sali, A., & Zamri, Z. A. 2014, *AJ*, **147**, 147
- Sodin, L. G., & Kopilovich, L. E. 2002, *A&A*, **392**, 1149
- Swarup, G., Ananthakrishnan, S., Kapahi, V. K., et al. 1991, *CSci*, **60**, 95
- Thompson, A. R., Moran, J. M., & Swenson, G. W. 2008, *Interferometry and Synthesis in Radio Astronomy* (2nd ed.; New York: Wiley)
- Torchinsky, S. A., Broderick, J. W., Gunst, A., et al. 2017, arXiv:1610.00683
- Woody, D. 2001a, *Radio Interferometer Array Point Spread Functions I. Theory and Statistics*, ALMA Memo No. 389
- Woody, D. 2001b, *Radio Interferometer Array Point Spread Functions II. Evaluation and Optimization*, ALMA Memo No. 390